Pseudopotential molecular-structure calculations for alkali-metal-atom—H_2 systems

F. Rossi and J. Pascale
Service de Physique des Atomes et des Surfaces, Commissariat à l'Energie Atomique, Centre d'Etudes Nucléaires de Saclay, 91191 Gif-sur-Yvette Cédex, France
(Received 22 April 1985)

Two-center molecular-structure calculations using an l-dependent pseudopotential technique have been performed for alkali-metal-atom—H_2 systems, and the adiabatic potential energies for the ground states and numerous excited states of these systems have been obtained for the $C_{\infty v}$ and C_{2v} symmetries. The H_2 molecule was assumed to lie in its ground state $X^1\Sigma_g^+(v=0)$ and its bond length fixed to the equilibrium value $r_e=1.4$ a.u. The interaction between the valence electron of the alkali-metal atom and H_2 is described by a one-center effective interaction which is modeled to reproduce differential elastic-scattering experimental data at low energies. The results are generally in good agreement with available *ab initio* calculations indicating the reliability and the usefulness of such an approach. The present calculations fill in the lack of information concerning most of these systems.

I. INTRODUCTION

Knowledge of the potential-energy surfaces is of great importance in understanding either quantitatively or qualitatively various reactive or nonreactive processes which may occur during collisions between electronically excited atoms and molecules. The purpose of this paper is to show that the semiempirical l-dependent pseudopotential method, which has been successfully used recently for the study of M-He interactions[1] (where M is an alkali-metal atom), can be also considered as a reliable method for treating the M-H_2 systems.

Molecular-structure calculations concerning the M-H_2 systems are rather few in number and often incomplete. Full *ab initio* calculations were performed for LiH_2 (Refs. 2—6) and NaH_2,[7,8] at various levels of sophistication, illustrating the complexity of this approach. More recently, the CsH_2 system has been investigated using an *ab initio* pseudopotential method.[9] Apart from these *ab initio* calculations, the LiH_2 (Ref. 10) and NaH_2 (Ref. 11) systems have been also investigated with the semiempirical diatomics-in-molecules (DIM) method based on information about the diatomic fragments. This method, while very useful for obtaining qualitative behavior of the potential-energy surfaces, does not seem to give sufficiently accurate results for the purpose of quantitative comparisons.

The *ab initio* methods for calculating the potential-energy surfaces have to solve a many-body problem independently of any experimental data. This problem, already very complex in the case of a diatomic molecule when the number of electrons is large, becomes tremendous for a triatomic molecule because of additional degrees of freedom to describe the system. The level of sophistication of such calculations depends upon the electronic configurations used to define the electronic wave function of the system, and then reliable results are generally obtained at the expense of large computational efforts. This precludes extensive calculations, and therefore the full *ab initio* potential-energy surfaces may be of limited use for calculating nonadiabatic coupling needed in the treatment of scattering problems. They may be very useful nevertheless as a guide or reference for a less rigorous approach of the many-body problem.

In order to shorten computational efforts required by full *ab initio* methods, the pseudopotential approach has been developed.[12] Because only a few valence electrons are generally responsible for chemical bonding, the many-body problem is reduced to the interactions between valence electrons and cores. Then, only the correlations between the valence electrons have to be explicitly included in the calculations, the interaction between a valence electron and a core being described by an effective potential. This effective potential may be built *ab initio*,[12] requiring the knowledge of the core orbitals. The semiempirical approach which consists in modeling the effective interaction in order to reproduce some experimental data seems easier to use for obtaining quite reliable results.[1]

In the present study of the M-H_2 systems we use an extension of the l-dependent pseudopotential approach previously used for the M-He systems.[1] However, a further simplification is made here by representing the interaction between the alkali valence electron e^- and H_2 by an effective one-center interaction which takes into account the anisotropy of the molecule. Our approach presents some analogies with that used by Bottcher[13] for NaN_2, but differs on the modelization of the effective interaction, the most important point being that our pseudopotential is energy independent. In Sec. II details on the effective interactions are given, as well as the method of calculation of the adiabatic potential energies. The results obtained for all the M-H_2 systems are reported and discussed in Sec. III with references to previous *ab initio* theoretical works. Finally, a general conclusion is given in Sec. IV.

II. METHOD OF CALCULATION

A. General framework

In the spirit of the semiempirical l-dependent pseudopotential approach previously used for the M-He systems,[1] the interaction between M and H_2 is reduced to a three-body system consisting of the alkali valence electron e^-, the alkali-metal-atom core A and H_2 considered as an anisotropic core B (see Fig. 1). The molecule H_2 is assumed to be in its ground state $X^1\Sigma_g^+(v=0)$. Therefore, our calculated adiabatic potential energies correspond to the equilibrium distance $r_e=1.4$ a.u. (atomic units will be generally used throughout the article) between the two hydrogen atoms.

Within the Born-Oppenheimer approximation, the problem of determining the adiabatic potential energies becomes the same as solving the one-electron Schrödinger equation

$$H_e\psi_e^{(i)}=\varepsilon_i(R,\gamma)\psi_e^{(i)} \tag{1}$$

for any given distance R between A and B (situated at the center of mass of H_2) and angle γ specifying the direction of the H_2-molecular axis with respect to the vector $\mathbf{R}$ taken as quantization axis (see Fig. 1), in order to obtain the electronic energy $\varepsilon_i(R,\gamma)$ for a given electronic state i. Then, the adiabatic potential energies $E_i(R,\gamma)$ are defined as

$$E_i(R,\gamma)=\varepsilon_i(R,\gamma)+V_{AB}(R,\gamma)\ , \tag{2}$$

where $V_{AB}(R,\gamma)$ is the potential describing the interaction between the two cores. The electronic Hamiltonian is defined as

$$H_e=-\tfrac{1}{2}\nabla_{\mathbf{r}_A}^2+V_A+V_B+V_{\mathrm{CT}}\ , \tag{3}$$

where V_A and V_B are, respectively, operators describing the e^--A and e^--B effective interactions. V_{CT} represents a three-body interaction (the so-called cross term) which has to be included in the calculations in order to have the correct behavior of $E(R,\gamma)$ at large R values. The spin-orbit interaction is not included in the present calculations. The $V_{A,B}$ interactions contain a short-range part which is described by an l-dependent pseudopotential, and a long-range part including polarization terms. As in Ref. 1, we take

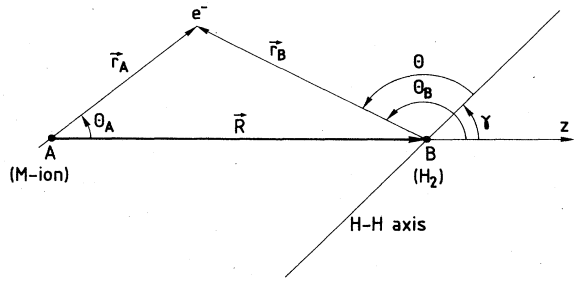

FIG. 1. Three-body two-center model for describing the M-H_2 interaction. The M ion is in A and the center of mass of H_2 is in B.

$$V_A=\sum_{l=0}^{\infty}V_{Al}(r_A)\mathscr{P}_l^A-\frac{1}{r_A}-\frac{1}{2}\frac{\alpha_{d_A}}{(r_A^2+d_A^2)^2}-\frac{1}{2}\frac{\alpha'_{q_A}}{(r_A^2+d_A^2)^3}\ , \tag{4}$$

where $\mathscr{P}_l^A$ is an angular momentum projector on center A and $V_{Al}(r_A)$ is a Gaussian-type potential. The values of the parameters defining $V_{Al}(r_A)$, as well as those of α_{d_A}, α'_{q_A}, and d_A were previously obtained by Bardsley.[12] Note that for $l\geq l_{\max}$, where $l_{\max}$ depends on the alkali-metal atom A, the radial operators V_{Al} are identical. Let us discuss now in more detail V_B and V_{CT}.

B. The effective interaction e^--H_2 and the cross term

The operator V_B describing the e^--H_2 interaction is written, as for V_A, as the sum of a short-range part and of a long-range part that we limit to terms in R^{-4}. But now, anisotropic terms are also included to take into account the molecular structure of H_2; to be consistent with the long-range part, we limit them to terms in $P_2(\cos\theta)$ for the short-range part, where θ is the angle between the molecular axis and $\mathbf{r}_B$ (see Fig. 1). Then,

$$V_B=\sum_{l=0}^{\infty}V_{Bl}^{(0)}(r_B)\mathscr{P}_l^B+\sum_{l=0}^{\infty}V_{Bl}^{(2)}(r_B)\tfrac{1}{2}\{P_2(\cos\theta),\mathscr{P}_l^B\}-\frac{1}{2}\frac{\alpha_{d_B}^{(0)}}{(r_B^2+d_B^2)^2}-\left[\frac{1}{2}\frac{\alpha_{d_B}^{(2)}r_B^2}{(r_B^2+d_B^2)^3}+\frac{Qr_B^3}{(r_B^2+d_B^2)^3}\right]\times P_2(\cos\theta)\ , \tag{5}$$

where the symbol $\{\ \}$ denotes an anticommutator. Because $P_2(\cos\theta)$ does not commute with the angular momentum projector $\mathscr{P}_l^B$, it is necessary to introduce the anticommutator in Eq. (5) to ensure the hermiticity of the anisotropic short-range operator. This can be easily verified if one notes that the action of the anticommutator on the electronic wave function is defined as

$$\{P_2(\cos\theta),\mathscr{P}_l^B\}\psi_{el}(\hat{\mathbf{r}}_B,r_B)=\sum_{m=-l}^{+l}Y_l^m(\hat{\mathbf{r}}_B)\int d\hat{\mathbf{r}}'_B[P_2(\cos\theta)+P_2(\cos\theta')]\times Y_l^{m*}(\hat{\mathbf{r}}'_B)\psi_{el}(\hat{\mathbf{r}}'_B,r_B) \tag{6}$$

with $\hat{\mathbf{r}}_B=\mathbf{r}_B/r_B$.

We consider first the short-range part of the interaction. It is described by a pseudopotential in analogy with the description of the e^--He short-range interaction.[1] As for the e^--He interaction, the role of the pseudopotential is also mainly to simulate the Pauli principle, and therefore it has to be l dependent. However, for e^--H_2, the l dependence of the pseudopotential is more difficult to formulate than for e^--He, in particular when e^- is near the core B. We have generalized the isotropic pseudopotential used for e^--He, by introducing an angular dependence in

θ, and using also the same Gaussian-type radial operators:

$$V_{Bl}^{(0,2)}(r_B)=A_l^{(0,2)}e^{-B_l^{(0,2)}r_B^2} . \quad (7)$$

This formulation allows us to take into account to a certain degree the l symmetry as the electron approaches H_2, and also gives us more flexibility to describe the correct e^--H_2 interaction.

The long-range part of the e^--H_2 interaction is relatively well-known.[14,15] We use the cutoff functions previously defined by Hara,[15] with the same cutoff radius $d_B=1.6$ a.u., to avoid any divergence of the terms for $r_B=0$. We have used the values $\alpha_{d_B}^{(0)}=5.1786$ a.u. and $\alpha_{d_B}^{(2)}=1.2019$ a.u. (Ref. 16) for the isotropic and anisotropic static dipole polarizabilities, respectively, and the value $Q=0.49$ a.u. (Ref. 17) for the quadrupole moment. These values correspond to H_2 in its ground state $X^1\Sigma_g^+(v=0)$. The e^--H_2 interaction defined above was then modeled in order to reproduce scattering experimental data. For this purpose, the differential cross sections for the e^--H_2 elastic scattering were calculated using the method developed by Takayanagi and Geltman.[18] This method was later used by Hara[15] and Sur and Ghosh,[19] but with different e^--H_2 interactions than used in Ref. 18 or in the present work. For a given set of parameters defining our e^--H_2 interaction, the phase shifts for each l wave (up to the f wave) were calculated from uncoupled radial equations, for three orientations of the H-H axis with respect to the quantization axis $(0,\Pi/4,\Pi/2)$. The averaged differential cross sections were then derived and compared with experimental data. In spite of unavoidable difficulties due to several parameters to adjust at the same time, we were able to reasonably reproduce the differential elastic scattering data of Linder and Schmidt[20] in the energy range 0.6—10 eV and the theoretical scattering length $L_0=1.27$ a.u. obtained by Chang,[21] by limiting the l dependence of the pseudopotential to $l=0,1$, as for the case of the e^--He interaction.[1] The calculated differential cross sections were sufficiently sensitive to the parameters to strongly indicate their variation limits. The best agreement with the experimental data, shown in Fig. 2, was obtained for $A_0^{(0)}=4.5$, $A_0^{(2)}=0$, $B_0^{(0)}=0.4$, $A_{l\geq 1}^{(0)}=-0.4$, $A_{l\geq 1}^{(2)}=-2.5$, $B_{l\geq 1}^{(0,2)}=0.4$.

Let us consider now the well-known cross term[22] resulting from the polarization of H_2 by both the point charges e^- and A. To be consistent with our choice of cutoff functions for the long-range part of the e^--H_2 interaction, the cross term was defined as

$$V_{\mathrm{CT}}=-\left[\frac{\alpha_{d_B}^{(0)}\cos(\theta_B)}{(R^2+d_B^2)(r_B^2+d_B^2)}+\frac{\alpha_{d_B}^{(2)}r_B R\,(3\cos\theta\cos\gamma-\cos\theta_B)}{2(R^2+d_B^2)^{3/2}(r_B^2+d_B^2)^{3/2}}\right]f_c\left[\frac{R}{r_A}\right], \quad (8)$$

where we have also included the additional cutoff function which was introduced and discussed previously for the M-He systems,[1]

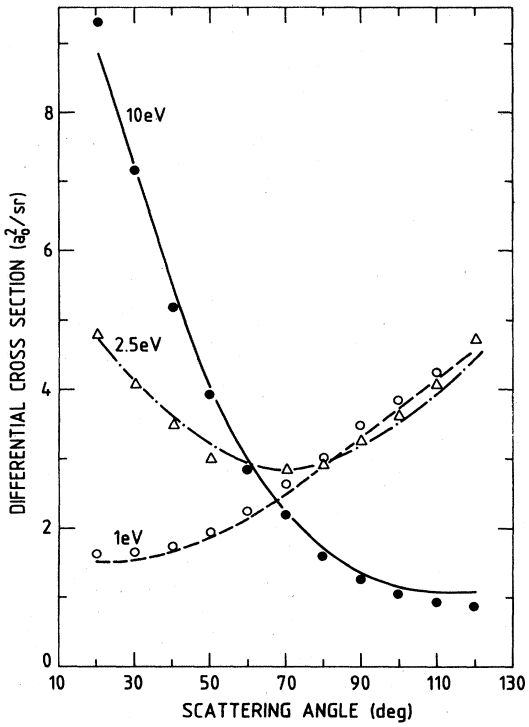

FIG. 2. Differential cross sections vs scattering angle for the elastic scattering of e^- by H_2 in its ground state $X^2\Sigma_g^+$ $(v=0)$, for three energies as indicated in the figure. The symbols are the experimental points of Linder and Schmidt (Ref. 20).

$$f_c(R/r_A)=\begin{cases}1-\exp\left[-\left[\dfrac{R}{r_A}-1\right]^2\right] & \text{for } R\geq r_A \quad (9a)\\ 0 \text{ for } R<r_A . & (9b)\end{cases}$$

Note that the anisotropic part of the cross term can be easily obtained by specifying the dipole polarizability tensor in terms of the components of the unit vector defining the orientation of the H_2-molecular axis.[14]

C. The alkali-ion—H_2 interaction

The long-range part of the alkali-ion—H_2 interaction can be easily derived.[14] Some information about the repulsive part of the potentials can be obtained from beam-scattering experiments.[23] However it is limited to only a small R-value range and the potentials derived from the scattering data are averaged over all orientations of the H_2-molecular axis. This latter point precludes the use of an extrapolation method, as the one used previously for the alkali-ion—He interactions,[1] to build the full potential curves for any symmetry of the system.

The method proposed here to estimate the alkali-ion—H_2 interaction $V_{AB}(R,\gamma)$ for any values of R and γ is prompted by a stationary perturbative approach used by Hara[15] to study the scattering of electrons by hydrogen molecules. We consider the interactions between the alkali-ion A and each point charge constituting the H_2

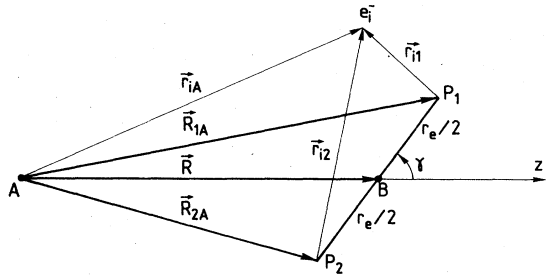

FIG. 3. Three-center model for describing the M-ion—H_2 interaction. The two protons p_1 and p_2 are placed symmetrically with respect to B at the distance $r_e=1.4$ a.u. from each other.

molecule: two protons p_i placed symmetrically with respect to the center of mass B and two electrons e_i^- (see Fig. 3). But here, the interactions are not only Coulombic, but include also a short-range part described by a pseudopotential. Thus, for the e_i^--A interaction we use an l dependent effective interaction

$$v_{iA}=\sum_{l=0}^{\infty} V_{Al}(r_{iA})\mathscr{P}_l^A-\frac{1}{r_{iA}} \tag{10}$$

and the p_i-A interaction is assumed to be local and described by

$$v_{P_iA}=-V_{Al_{\max}}(R_{iA})+\frac{1}{R_{iA}}\ , \tag{11}$$

where the V_{Al} radial operators are those defined in Eq. (4). The first-order term of the stationary perturbative method, which gives us the electrostatic potential, is just the average value of the sum of the interactions v_{iA} and v_{P_iA} with respect to the ground-state wave function of the H_2 molecule. In order to evaluate this term, the Coulombic part of the interactions can be expanded in terms of Legendre polynomials $P_l(\cos\gamma)$. Then it can be seen that only even terms will contribute to the static potential. Moreover, it can be shown also that the term in $P_2(\cos\gamma)$ of the Coulombic interactions corresponds asymptotically to the quadrupole interaction. As previously done by Hara,[15] we use a linear combination of atomic orbitals (LCAO) approximation for the ground-state wave function of H_2:

$$\Phi_{12}=\varphi_1\varphi_2 \tag{12}$$

with

$$\varphi_i=\frac{1}{\sqrt{2(S+1)}}\sum_{j=1}^{2}\left[\frac{\delta^3}{\pi}\right]^{1/2}e^{-\delta r_{ij}} \tag{13}$$

and where S is the overlap of the normalized Slater orbitals describing the two-center one-electron wave function φ_i with the value of δ optimized for H_2 ($\delta=1.166$).[15] Then, because Φ_{12} leads to an underestimation of the value of the quadrupole moment ($Q_{\text{calc}}=0.32$ a.u.) we have calculated the electrostatic potential by considering the short-range parts of the interactions v_{iA} and v_{P_iA} and retaining only the terms in $P_0(\cos\gamma)$ of the Legendre polynomial expansion of the Coulombic parts of the interactions. This defines V'_{static}. The full static potential is obtained by adding consistently with Eq. (5) the quadrupole contribution to the alkali-ion—H_2 interaction:

$$V_{\text{static}}(R,\gamma)=V'_{\text{static}}(R,\gamma)+\frac{QR^3}{(R^2+d_B^2)^3}P_2(\cos\gamma)\ . \tag{14}$$

We have verified that the terms in $P_4(\cos\gamma)$ of the Coulombic interaction expansion are very small for any value of R with respect to terms in P_0 and P_2, and therefore they have been neglected.

Finally, to obtain the full potential $V_{AB}(R,\gamma)$ describing the ground state of the alkali-ion—H_2 systems, we add to $V_{\text{static}}(R,\gamma)$ the induction energy, consistently with the expressions previously defined for the e^--H_2 interaction [see Eq. (5)]

$$V_{\text{induction}}(R,\gamma)=-\frac{\alpha_{d_B}^{(0)}}{2(R^2+d_B^2)^2}-\frac{\alpha_{d_B}^{(2)}R^2}{2(R^2+d_B^2)^3}P_2(\cos\gamma) \tag{15}$$

as well as the dispersion energy

$$V_{\text{dispersion}}(R,\gamma)=-\tfrac{3}{2}F\left[\frac{\alpha_{d_A}\alpha_{d_B}^{(0)}}{(R^2+d_A^2)^{3/2}(R^2+d_B^2)^{3/2}}+\frac{1}{2}\frac{\alpha_{d_A}\alpha_{d_B}^{(2)}R^2P_2(\cos\gamma)}{(R^2+d_A^2)^2(R^2+d_B^2)^2}\right]. \tag{16}$$

We use the Slater-Kirkwood formula[24] for estimating the factor F in Eq. (16) and take

$$F=\left[\left[\frac{\alpha_{d_A}}{N_A}\right]^{1/2}+\left[\frac{\alpha_{d_B}^{(0)}}{N_B}\right]^{1/2}\right]^{-1}\ , \tag{17}$$

where N_A (N_B) is the number of electrons in the core A (B). With the expressions defined above for the long-range parts of e^--H_2 and A-H_2 interactions and also that of the cross term [see Eq. (8)], the adiabatic potential energies have the correct asymptotic behavior up to terms in R^{-6}. Defining $V_i(R,\gamma)=E_i(R,\gamma)-E_i(\infty,\gamma)$, one has

$$V_i(R,\gamma)=-\frac{6Q}{R^5}[\langle r_A^2P_2(\cos\theta_A)\rangle_i P_2(\cos\gamma)+\tfrac{1}{8}C_i\sin^2\gamma-2D_i\cos\gamma\sin\gamma]-\frac{\alpha_{d_B}^{(0)}}{R^6}\{\langle r_A^2[P_2(\cos\theta_A)+1]\rangle_i+\tfrac{3}{2}F\alpha_{d_A}\}$$
$$-\frac{\alpha_{d_B}^{(2)}}{2R^6}(\{\langle r_A^2[3P_2(\cos\theta_a)+1]\rangle_i+\tfrac{3}{2}F\alpha_{d_A}\}P_2(\cos\gamma)+\tfrac{3}{4}C_i\sin^2\gamma-6D_i\cos\gamma\sin\gamma)\quad\text{for } R\to\infty\ , \tag{18}$$

where C_i and D_i are defined as

$$C_i = \langle r_A^2 \sin^2\theta_A \cos 2\varphi \rangle_i \ , \tag{19a}$$

$$D_i = \langle r_A^2 \sin\theta_A \cos\theta_A \cos\varphi \rangle_i \ , \tag{19b}$$

and $\langle \ \rangle_i$ denotes the average value with respect to the wave function of the alkali-metal atom in the state i. Note that only the quadrupole interaction due to H_2 gives a R^{-5} asymptotic behavior of $V_i(R,\gamma)$ and only if the molecular state correlating with the state i of the alkali-metal atom is not an nS state. This quadrupole interaction does not contribute to the order R^{-6}. The coefficients C_i and D_i take into account the azimuthal orientation φ of $\mathbf{r}_A$ with respect to the plan formed by the core A and the direction H-H of the molecule. This asymptotic expression will be useful later on in this article when discussing the behavior of the adiabatic potential curves.

Because the present study concerns the interactions of the M-H_2 systems in the $C_{\infty v}$ and C_{2v} symmetries, we have also limited to the same symmetries our calculations of the alkali-ion—H_2 interaction potentials. However, it is straightforward to extend to the general C_s symmetry the calculations of the alkali-ion—H_2 interactions using the method described above. Finally, it is also worthwhile noting that this method could be used for other systems; in particular, some preliminary calculations on alkali-ion—He systems have demonstrated to us the usefulness of the method for obtaining reliable results.

D. Molecular-structure calculations

The molecular code previously used for the M-He systems[1] has been adapted in order to calculate the matrix elements of the additional anisotropic terms involved in the case of the M-H_2 interactions, allowing us to calculate the electronic energies $\varepsilon_i(R,\gamma)$. Again, as in Ref. 1, the molecular wave function $\psi_e^{(i)}(\mathbf{r}_A,\mathbf{R},\gamma)$ was expanded over the same large basis set of Slater-type orbitals (STO) centered on the alkali ion, and ensuring the stability of the calculated electronic energies up to corresponding highly excited states of the alkali-metal atom. We recall that the nonlinear parameters of the STO were optimized in order to reproduce accurately the ionization energies of the excited states up to first nG state (in general, the accuracy is much better than 2.5×10^{-4} a.u.).[1] Our basis set is sufficiently flexible to take implicitly into account at short distances the coupling with the ionic term associated with the alkali-ion—H_2^- systems, but is obviously unable to predict the energies of these ionic systems.

In the present work, we have limited our calculations to the $C_{\infty v}$ and C_{2v} symmetries of the systems. However, the calculations could be extended to the C_s symmetry provided that the molecular code is adapted accordingly. For each symmetry, all the adiabatic potential energies correlating with a particular alkali-metal-atom state were calculated. In the $C_{\infty v}$ symmetry, the classification of the adiabatic potential-energy curves is identical to that for the M-He systems, and the electronic terms result from a diagonalization of the one-electron Hamiltonian for each value of the projection M_L of the total orbital momentum $\mathbf{L}$ (equal to that of the valence electron, in the present case). In the C_{2v} symmetry, the adiabatic potential energy are classified as usually done,[25] in four classes of electronic terms (namely, the classes A_1, B_1, B_2, and A_2). Each class of electronic terms results from a different diagonalization of the electronic Hamiltonian. It is useful to say here that $\frac{1}{4}[2l+3+(-1)^l]$, $\frac{1}{4}[2l-1+(-1)^l]$, and $\frac{1}{4}[2l+1-(-1)^l]$ terms of classes A_1, A_2, and B_1 (B_2) arise, respectively, from a given nl level of the M atom.

TABLE I. Characteristic parameters for the ground-state potential of Li^+H_2 in the $C_{\infty v}$ and C_{2v} symmetries: position R_{eq} (in a.u.) and depth D_{eq} (in eV) of the potential well; position R_a (in a.u.) and height E_a (in eV) of the long-range potential barrier found in the $C_{\infty v}$ symmetry. Comparison with previous *ab initio* calculations at various levels of approximation.

Symmetry		Present	a	b	c	d	e	f
$C_{\infty v}$	R_{eq}	4.85	~4.75	4.7 (4.7)				
	D_{eq}	1.77×10^{-2}	$\sim4.0\times10^{-2}$	4.63×10^{-2} (6.47×10^{-2})				
	R_a	9.1	~9.5	~9.75 (~11.5)				
	E_a	4.3×10^{-3}	4.0×10^{-3}	3.8×10^{-3} (3.0×10^{-3})				
C_{2v}	R_{eq}	3.88	~4.0	3.75 (3.75)	3.912	4.21	3.99	4.25
	D_{eq}	1.75×10^{-1}	$\sim2.4\times10^{-1}$	2.50×10^{-1} (2.53×10^{-1})	2.25×10^{-1}	1.93×10^{-1}	2.02×10^{-1}	1.64×10^{-1}

[a]Hartree-Fock self-consistent-field (HF-SCF) calculations of Lester (Ref. 26).
[b]HF calculations of Kutzelnigg *et al.* (Ref. 27) using the independent-electron-pair-approximation—pair-natural-orbital (IEPA-PNO) method with or without (in parentheses) correlation energy.
[c]HF-SCF calculations of Raffenetti and Ruedenberg (Ref. 28).
[d]Unrestricted Hartree-Fock—unrestricted Moller-Plesset second-order perturbation approximation (using a standard basis set of Gaussian orbitals designated by 6-31G**) (HF-UMP2/6-31G**) calculations of of Collins *et al.* (Ref. 29).
[e]HF/6-31G** calculations of Hobza and Schleyer (Ref. 30).
[f]*ab initio* model potential calculations of Switalski *et al.* (Ref. 31).
[g]$1.77\times10^{-2}=1.77\times10^{-2}$.

TABLE II. Characteristic parameters (as in Table I) of the ground-state potentials of the alkali-ion—H_2 systems in the $C_{\infty v}$ and C_{2v} symmetries obtained from the present calculations, and from the *ab initio* calculations of Raffenetti and Ruedenberg (Ref. 28) (a) and of Switalski *et al.* (Ref. 30) (b) in the case of Na^+H_2.

Symmetry	Alkali ion	Na^+			K^+	Rb^+	Cs^+
		Present	(a)	(b)			
$C_{\infty v}$	R_{eq}	5.75			6.95	7.18	7.7
	D_{eq}	4.63×10^{-3}			2.7×10^{-5}	1.22×10^{-4}	6.8×10^{-4}
	R_a	9.3			10.1	10.5	11.1
	D_a	4.2×10^{-3}			3.6×10^{-3}	3.3×10^{-3}	2.9×10^{-3}
C_{2v}	R_{eq}	4.68	4.705	5.20	5.75	6.11	6.53
	D_{eq}	1.08×10^{-1}	1.25×10^{-1}	7.8×10^{-2}	6.29×10^{-2}	5.43×10^{-2}	4.65×10^{-2}

III. RESULTS AND DISCUSSIONS

Calculations were performed on all the M-H_2 systems for distances R between 2 and 50 a.u., and the adiabatic potential energies corresponding to the ground state and numerous excited levels of the M atom were obtained for the $C_{\infty v}$ and C_{2v} symmetries. Only some examples of our calculations will be shown, but tabulated energies will be available upon request from the authors. Because information on the alkali-ion—H_2 systems is presently available only for Li^+H_2 and Na^+H_2, let us first discuss our results concerning the alkali-ion—H_2 interaction potentials before considering the M-H_2 systems. We recall that all our calculations were performed with the characteristic parameters of H_2 corresponding to a distance between the two protons fixed at $r_e = 1.4$ a.u.

A. Alkali-ion—H_2 systems

The characteristic parameters of the ground-state interaction potentials for the alkali-ion—H_2 systems that we have obtained are reported in Tables I and II along with previous *ab initio* results, when available.[6,26–30] The Li^+H_2 system has been investigated by full *ab initio* methods,[6,26–29] at various levels of approximation which are difficult to analyze here. In spite of the simplicity of our method of calculating $V_{AB}(R,\gamma)$, the agreement with the *ab initio* calculations is satisfactory (see Table I). The position of the potential well is correctly predicted, while the well depth is slightly underestimated with respect to the full *ab initio* results. It is worthwhile noting that in the $C_{\infty v}$ symmetry, our predictions concerning the small potential barrier observed at large R is in close agreement with the full *ab initio* calculations of Lester,[26] and those of Kutzelnigg *et al.*[27] when the correlation energy is not considered. Note in this connection that for such small potential energies, inclusion of the correlation energy is a very delicate problem. Figure 4 shows as an example the overall agreement with the full *ab initio* calculations of Lester[26] that we have obtained for the potential-energy curves of Li^+H_2 in the $C_{\infty v}$ and C_{2v} symmetries. For Na^+H_2 in the C_{2v} symmetry, our predictions concerning the well depth of the potential curve are in closer agreement with the full *ab initio* calculations of Raffenetti and Ruedenberg[28] than are the *ab initio* model potential calculations of Switalski *et al.*[30] Our calculations predict decreasing potential well depths and potential barriers heights when going from Li^+H_2 to Cs^+H_2, and located accordingly at larger and larger distances (see Table II). It is interesting to note that the well depths of the potentials in the C_{2v} symmetry, are larger by about a factor of 3 to 10 than those found for the corresponding alkali-ion—He system (see Table II of Ref. 1, for example), but the situation is reverse in the case of the $C_{\infty v}$ symmetry where the potential wells are found to be much less deep. This can be explained as being a result of the opposing contributions of the quadrupole interaction due to H_2 [see Eq. (14)], which is the main term at large distances.

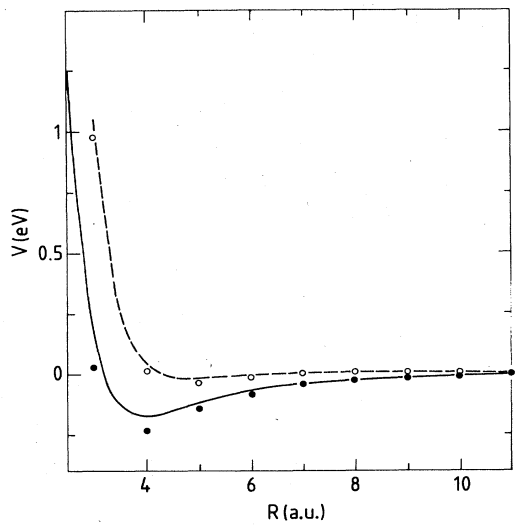

FIG. 4. Interaction potential $V(R)$ for the ground state of Li^+H_2. $C_{\infty v}$ symmetry: — — —, present results; ○, HF-SCF calculations of Lester (Ref. 26). C_{2v} symmetry: ——, present results; ●, HF-SCF calculations of Lester (Ref. 26).

B. LiH_2 system

Our results for the ground state and the first excited states of LiH_2 in the $C_{\infty v}$ and C_{2v} symmetries are shown, respectively, in Figs. 5 and 6 along with *ab initio* calculations.[2,4] Note that the Hartree-Fock (HF) results of Krauss[2] refer to a distance between the two hydrogen atoms of $R_{H\text{-}H} = 1.5$ a.u. However, in view of the depen-

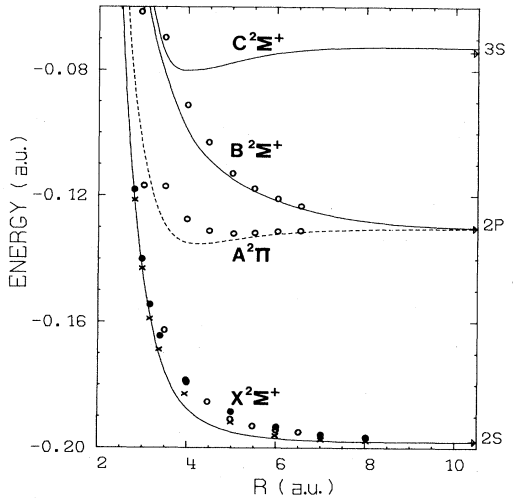

FIG. 5. Adiabatic potential energies of the lowest states of LiH_2 in $C_{\infty v}$ symmetry. Present results compared with the HF calculations of Krauss (Ref. 2), o, and with the MCSCF-OVC calculations of Wagner *et al.* (Ref. 4) for two levels of approximation (×, 15 OVC and ●, 28 OVC). The *ab initio* potential curves have been correlated asymptotically to the experimental levels for meaningful comparisons with our results. Arrows indicate the position of the asymptotic energies.

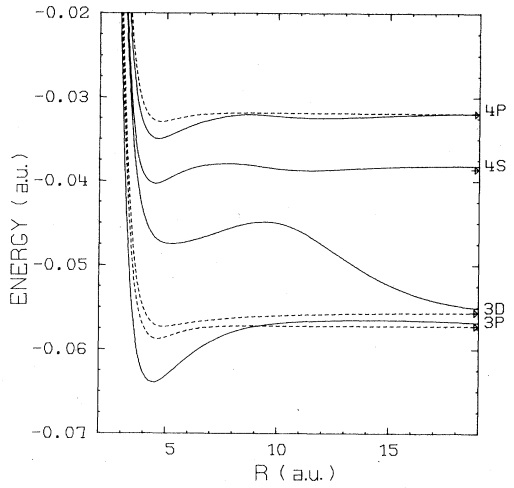

FIG. 7. Adiabatic potential energies of some excited states of LiH_2 in $C_{\infty v}$ symmetry. ——, $^2\Sigma^+$; — — —, $^2\Pi$ states; the other curves ($^2\Delta$, etc.) have not been drawn for the clarity of the figure.

dence of the adiabatic potential energies on $R_{H\text{-}H}$,[2] the changes for $R_{H\text{-}H}=1.4$ a.u. should be small and the comparisons with our results remain meaningful. Moreover, these are the only extensive results concerning the excited states which are available for a systematic comparison with our results. The results of Wagner *et al.*[4] obtained for the ground state from more sophisticated calculations [multiconfiguration self-consistent-field—optimized-valence-configuration (MCSCF-OVC) method] are presented for two levels of approximation (15 OVC and 28 OVC) illustrating the difficulty for correctly taking into account the correlation effects, in particular at large and intermediate distances. Their results in the $C_{\infty v}$ symmetry indicate a steeper repulsive curve than ours. The agreement on the whole is good, in particular for the C_{2v} symmetry. We find, in agreement with previous *ab initio* calculations,[6] that the $X^2\Sigma^+$ potential presents a well ($D_{eq}=3.9\times10^{-3}$ eV, $R_{eq}=9$ a.u.) which is deeper than for the X^2A_1 potential ($D_{eq}=1.73\times10^{-3}$ eV, $R_{eq}=12.0$ a.u.). Concerning the excited states, our results for the C_{2v} symmetry are in better agreement with those of Krauss[2] than are the results for the $C_{\infty v}$ symmetry. The characteristic parameters of our A^2B_2 potential curve are $D_{eq}=0.61$ eV, $R_{eq}=3.3$ a.u. Comparatively Krauss[4] has

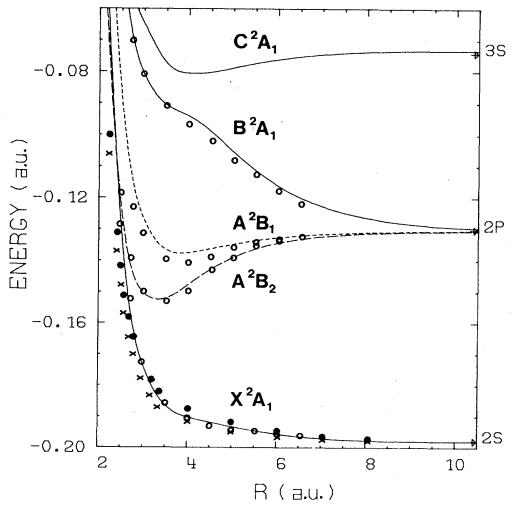

FIG. 6. Adiabatic potential energies of the lowest states of LiH_2 in C_{2v} symmetry, as in Fig. 5.

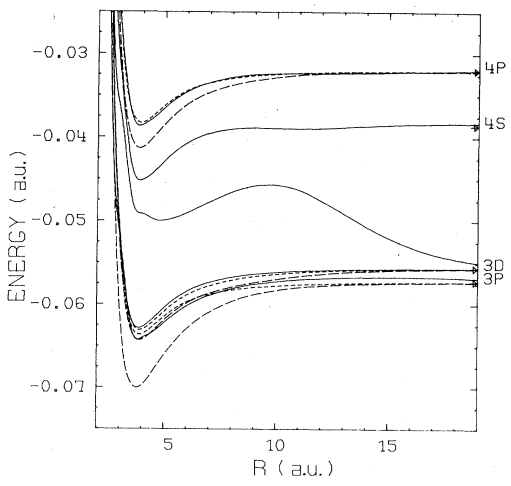

FIG. 8. Adiabatic potential energies of some excited states of LiH_2 in C_{2v} symmetry. ——, $^2A_1$; — — —, $^2B_1$; ——, $^2B_2$. The $^2A_2$ potential curves, which are very close to the lowest $^2A_1$ potential curves correlating asymptotically with the same levels, have not been drawn for the clarity of the figure.

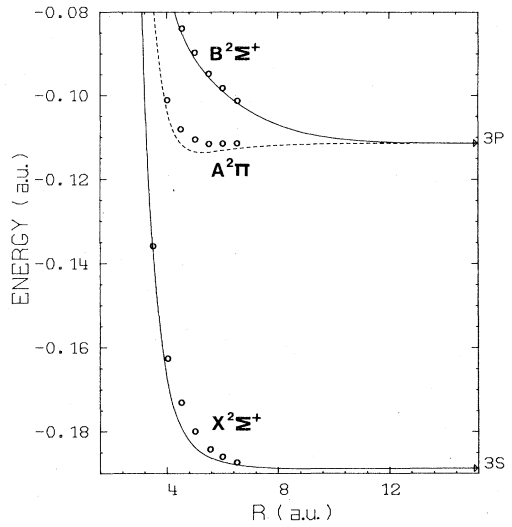

FIG. 9. Adiabatic potential energies of the lowest states of NaH_2 in $C_{\infty v}$ symmetry. Present results compared with the RHF-SCF calculations of Botschwina *et al.* (Ref. 7), ○.

found $D_{eq}=0.62$ eV, $R_{eq}=3.3$ a.u. The MCSCF-OVC calculations of Mizutani *et al.*[5] give $D_{eq}=0.41$ eV, $R_{eq}=3.5$ a.u.; and the Hartree-Fock (using a standard basis set of Gaussian orbitals designated by 6-31G**) (HF/6-31G**) calculations of Hobza and von Schleyer,[6] supposed to be more accurate than those of Mitzutani *et al.*,[5] find $D_{eq}=0.71$ eV, $R_{eq}=3.22$ a.u. Taking into account the fact that all these *ab initio* calculations were performed for $R_{H\text{-}H}=1.5$ a.u., which was found to give an absolute minimum in the A^2B_2 potential curve,[5,6] the value that we have found for D_{eq} at $R_{H\text{-}H}=1.4$ a.u. is quite reasonable. The most striking point of our calculations is to find that the X^2A_1 potential curve crosses the A^2B_2 potential curve at a distance $R=2.35$ a.u., with a corresponding activation energy $E_a\simeq 0.77$ eV relative to the 3^2P level. This result is in good agreement with the calculations of Krauss.[2] However, the shoulder observed in our B^2A_1 potential curve (see Fig. 6), due to coupling with the C^2A_1 state, was not found in the calculations of Krauss, perhaps because of the reduced basis set involved in his calculations. Finally, in Figs. 7 and 8 we show our predictions concerning the excited adiabatic potential curves for the $C_{\infty v}$ and C_{2v} symmetries.

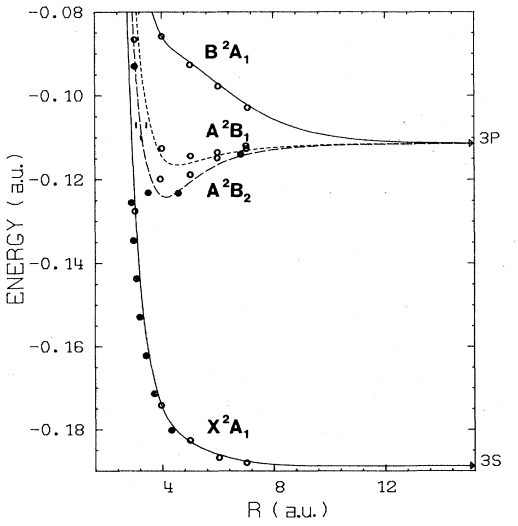

FIG. 10. Adiabatic potential energies of the lowest states of NaH_2 in C_{2v} symmetry. Present results compared with the RHF-SCF (○) and PNO-CEPA (●) calculations of Botschwina *et al.* (Ref. 7).

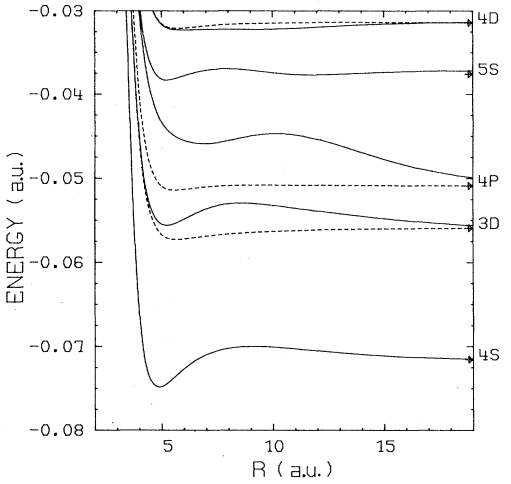

FIG. 11. Adiabatic potential energies of some excited states of NaH_2 in $C_{\infty v}$ symmetry, as in Fig. 7.

C. NaH_2 system

Figures 9 and 10 present the comparison between our results and the ones obtained by Botschwina *et al.*[7] from extensive *ab initio* calculations at two levels of approximation [using either the restricted Hartree-Fock self-consistent-field (RHF-SCF) method or the pair-natural-orbital—coupled-electron-pair-approximation (PNO-

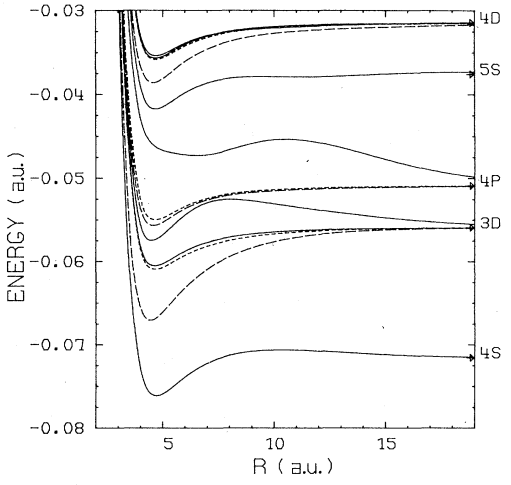

FIG. 12. Adiabatic potential energies of some excited states of NaH_2 in C_{2v} symmetry, as in Fig. 8.

CEPA) method; the second method in the most accurate but was only used to obtain the X^2A_1 and A^2B_2 potential curves]. The agreement with the PNO-CEPA results is quite good, with our X^2A_1 potential curve slightly more repulsive and our A^2B_2 potential curve slightly less attractive than that obtained from the PNO-CEPA calculations. In comparison, our results agree well with the RHF-SCF calculations for the X^2A_1 and B^2A_1 potentials, but our A^2B_1 and A^2B_2 potentials are more attractive than those of the RHF-SCF method. This result may be explained by the fact that some important correlations effects are not taken into account in the RHF-SCF calculations as they are in the PNO-CEPA method. These correlation effects are probably less important for the B^2A_1 state for which the potential curve is rapidly repulsive. The characteristic parameters for the A^2B_2 potential curve, which is the most attractive one, are $D_{eq}=0.348$ eV and $R_{eq}=4.08$ a.u. in our calculations; the PNO-CEPA results[7] give $D_{eq}=0.39$ eV and $R_{eq}=3.88$ a.u. for $R_{H\text{-}H}=1.4$ a.u. In comparison, the recent restricted-Hartree-Fock — self-consistent-field — configuration-interaction (RHF-SCF-CI) calculations of Sevin and Chaquin[8] agree well with the RHF-SCF calculations of Botschwina *et al.*[7] to determine an absolute minimum of the A^2B_2 potential curve for $R_{H\text{-}H}=1.42$ a.u. with $D_{eq}=0.25$ eV and $R_{eq}=4.16$ a.u., but are far from the PNO-CEPA results[7] which find the absolute minimum for $R_{H\text{-}H}=1.49$ a.u. with $D_{eq}=0.43$ eV and $R_{eq}=3.92$ a.u. Finally, we discuss the most recent DIM calculations of Blais *et al.*,[11] since their surface have been used for extensive dynamics calculations. Their X^2A_1 potential curve is found to be more repulsive for $R\gtrsim 4$ a.u., and their A^2B_2 potential well less deep ($D_{eq}\simeq 0.24$ eV, $R_{eq}\simeq 4.6$ a.u. for $R_{H\text{-}H}=1.4$ a.u.) than in our calculations and those of the PNO-CEPA method.[7] The results of the DIM calculations are, however, in quite good agreement with ours and those of the RHF-SCF calculations[7] for the B^2A_1 potential curve. But, the results of the DIM calculations differ markedly from ours and the *ab initio* ones[7,8] by predicting the existence of a B^2B_2 potential curve, of ionic character, which crosses the B^2A_1 potential curve at $R\simeq 5$ a.u. and exhibits an avoided crossing with the A^2B_2 potential curve at $R\simeq 3.5$ a.u.

In the case of the $C_{\infty v}$ symmetry, our results are in fair agreement with the RHF-SCF calculations[7] and, as expected from the results obtained for the C_{2v} symmetry, our $A^2\Pi$ potential well is found to be deeper than the *ab initio* one. In the case of the $B^2\Sigma^+$ potential curve, which is rapidly repulsive, our results are again in good agreement with the RHF-SCF calculations. Our predictions concerning more excited adiabatic potential curves are finally shown in Figs. 11 and 12.

D. KH_2, RbH_2, and CsH_2 systems

Figures 13—18 present some of our results for the K, Rb, and Cs-H_2 systems in the $C_{\infty v}$ and C_{2v} symmetries. Unfortunately, there is neither experimental nor theoretical information concerning KH_2 and RbH_2 for comparisons with our results. Recently, the CsH_2 system has been investigated by Gadea *et al.*[9] using an *ab initio* pseudopotential method and some preliminary results have been reported. According to the authors, Fig. 2 of their article shows only a qualitative picture of several $^2A_1$ and $^2B_2$ potential curves, making a quantitative comparison with their results meaningless. We simply remark that qualitatively one observes similar features in the excited potential-energy curves, with some avoided crossings between the potential curves which are found more pronounced in their calculations than in ours. In general, the potential energies obtained from these *ab initio* pseudopotential calculations are much lower than ours; in particular, the crossing observed between the B^2A_1 and B^2B_2 potential curves (see Fig. 18) is found located just above the 6^2P level in the calculations of Gadea *et al.*,[9] at about $R=6$ a.u., while it is found located above the 5^2D level in our calculations, at about $R=4.6$ a.u.

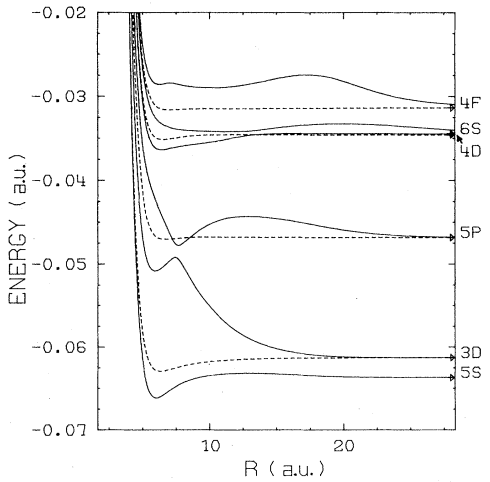

FIG. 13. Adiabatic potential energies of some excited states of KH_2 in $C_{\infty v}$ symmetry, as in Fig. 7.

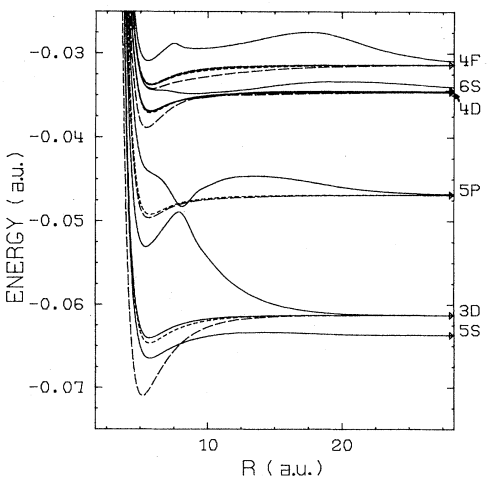

FIG. 14. Adiabatic potential energies of some excited states of KH_2 in C_{2v} symmetry, as in Fig. 8.

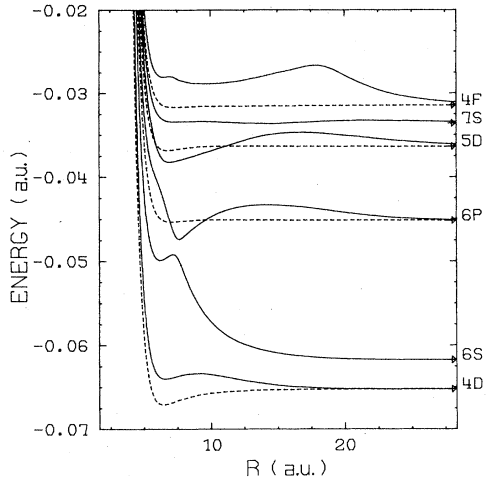

FIG. 15. Adiabatic potential energies of some excited states of RbH_2 in $C_{\infty v}$ symmetry, as in Fig. 7.

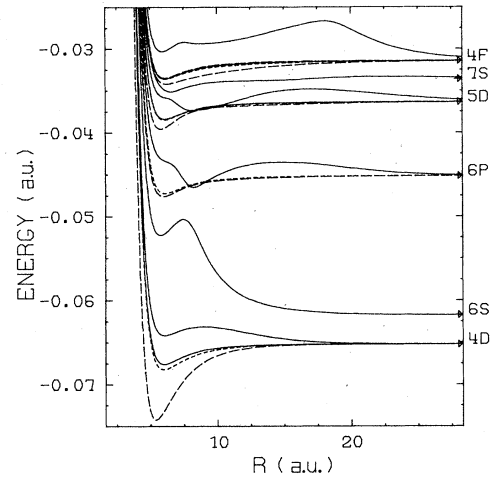

FIG. 16. Adiabatic potential energies of some excited states of RbH_2 in C_{2v} symmetry, as in Fig. 8.

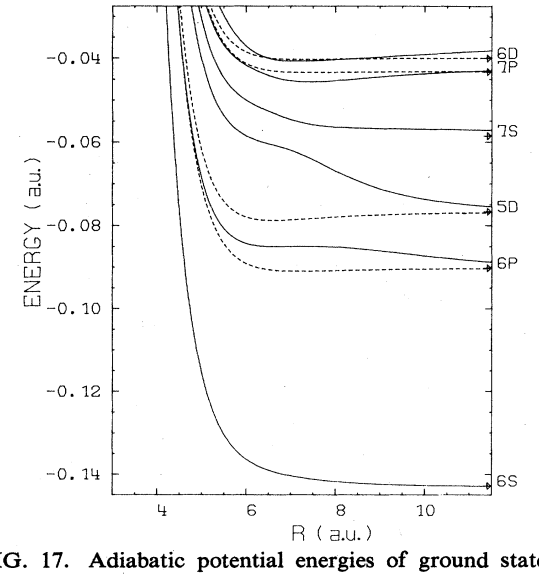

FIG. 17. Adiabatic potential energies of ground state and some excited states of CsH_2 in $C_{\infty v}$ symmetry, as in Fig. 7.

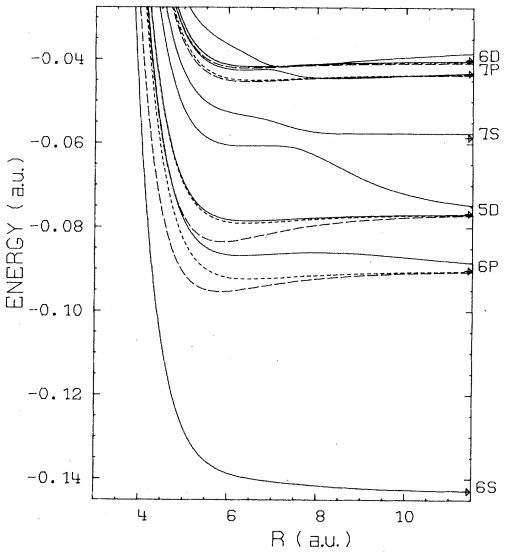

FIG. 18. Adiabatic potential energies of ground state and some excited states of CsH_2 in C_{2v} symmetry, as in Fig. 8.

E. General discussion of our results for the M-H_2 systems

Some structure is observed in the potential-energy curves for the excited states of the M-H_2 systems in the $C_{\infty v}$ and C_{2v} symmetries shown in Figs. 7, 8, and 11—18. It is similar to that which was previously observed in the potential-energy curves of the M-He systems,[1] but the main differences are generally observed at the avoided crossing between adiabatic potential curves. For the M-

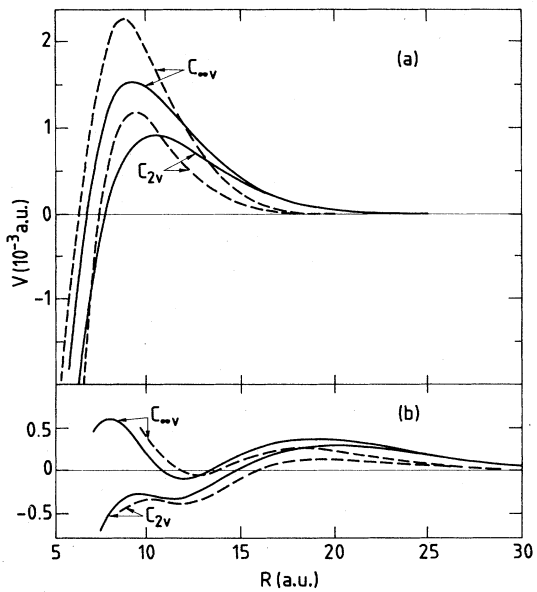

FIG. 19. Interaction potential of Na(nS) with H_2 for the $C_{\infty v}$ and C_{2v} symmetries as indicated in the figure, for $n=4$ (a) and $n=5$ (b). ——, present results; — — —, results of Ivanov (Ref. 32) obtained from an asymptotic method.

H_2 systems, these avoided crossings are more or less accentuated depending on the symmetry of the system. Moreover, some crossing may occur between some $^2A_1$ and $^2B_2$ potential curves correlating with different M-atom levels, at intermediate distances, due to much lower adiabatic potential energies obtained for a $^2B_2$ state than for the other molecular states associated with a given M atomic level. This is not observed correspondingly between the $^2\Sigma^+$ and $^2\Pi$ potential curves of the $C_{\infty v}$ symmetry, or in the case of the corresponding situation for the M-He system. See, for example, Figs. 13 and 14, where the crossing observed at $R \simeq 7.8$ a.u. between the $^2B_2(3^2D)$ and $^2A_1(5^2S)$ potential curves of KH_2 is not seen between the $^2\Pi(3^2D)$ and $^2\Sigma^+(5^2S)$ potential curves. Therefore, very different coupling between molecular states may result, depending on the symmetry (see, for example, Ref. 11 and references therein). Consequently, we would like to emphasize the point that it might be very audacious to use data for the M-He systems in order to interpret some nonreactive M-H_2 scattering processes; this was usually done in the past because of the lack of information concerning the M-H_2 potential surfaces. It is worthwhile noting that it is only for the C_{2v} symmetry that the ground-state potential curve is found to cross the first excited potential curve (that is the A^2B_2 curve), except for the case of KH_2. And it is only for LiH_2 that the activation energy at this crossing is found to be low, making the crossing visible in Fig. 6. Finally some of the structure observed in the excited potential curves in the range from intermediate to large distances is due to oscillations in the electronic wave function $\psi_e(\mathbf{r}_A,\mathbf{R},\gamma)$. As in the case of the M-He systems,[1] the adiabatic potential energy $V_i(R,\gamma)$ measured relative to its asymptote may be also estimated for the M-H_2 systems from an asymptotic method by considering the scattering of a free electron by the hydrogen molecule.[31] In Fig. 19 we show the comparison between our results and those obtained from such an approach[32] in the case of NaH_2, both for the $^2\Sigma^+$ and $^2A_1$ potential curves correlating with the 4^2S and 5^2S states of Na. The agreement, while qualitative, is, however, rather good over a large range of R values and indicates that such an asymptotic method could be quite useful for investigating high Rydberg states of the M-H_2 systems.

In Figs. 20–23 the adiabatic potential-energy curves $V_i(R,\gamma)$ relative to their asymptotes are reported for all the M-H_2 systems in the $X^2\Sigma^+$, X^2A_1, $B^2\Sigma^+$, B^2A_1, $A^2\Pi$, A^2B_1, and A^2B_2 states, allowing us to see the evolution of these curves when going from Li to Cs, or from the $C_{\infty v}$ symmetry to the C_{2v} symmetry. As in the case of the M-He systems,[1] one observes that for a given symmetry the repulsive strength of the same potential curve increases from Li to Cs, due to a more compressed wave function in the case of the lightest M atoms; and the order of the repulsive strengths is also changed for the $B^2\Sigma^+$ and B^2A_1 states due to coupling with the immediate upper state. Again, the $B^2\Sigma^+$ (B^2A_1) potential curve is more rapidly repulsive than the $X^2\Sigma^+$ (X^2A_1) potential curve, while the $A^2\Pi$, A^2B_1, and A^2B_2 potential curves present deeper wells when going from Cs to Li. The behavior of the potential curves with respect to each other, and with respect to the symmetry, $C_{\infty v}$ or C_{2v}, may be explained in terms of electronic densities. We can also explain the behavior of the potential curves in the range from large to intermediate distances by considering the asymptotic expression for $V_i(R,\gamma)$ [see Eq. (18)]. From such a study, we obtain the following results. The $X^2\Sigma^+$ and X^2A_1 potential curves are both attractive in R^{-6}, with the same contribution in $\alpha_{d_B}^{(0)}$, but the attractive strength of the X^2A_1 potential curve is reduced by the term in $\alpha_{d_B}^{(2)}$. At shorter distances, the repulsive strengths of the curves are mainly determined by the alkali-ion–H_2 interactions, and the $X^2\Sigma^+$ potential curves become more rapidly repulsive than the X^2A_1 ones. This is particularly clear from the X^2A_1 potential curve of LiH_2 (see Fig. 20) where an abrupt change in the repulsive strength of the

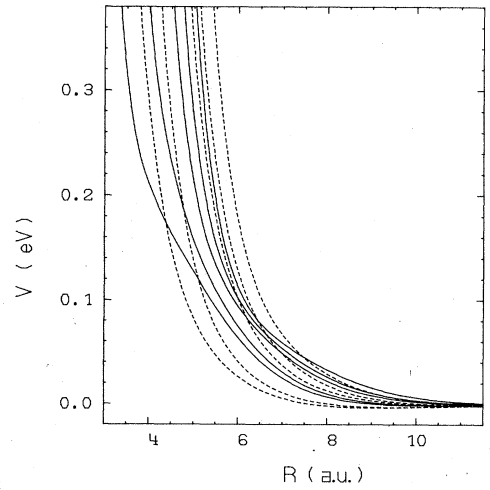

FIG. 20. Interaction potential $V(R)$ for the ground state of the M-H_2 systems. — — —, $X^2\Sigma^+$; ——, X^2A_1. The repulsive strength of the potential curve increases from Li to Cs.

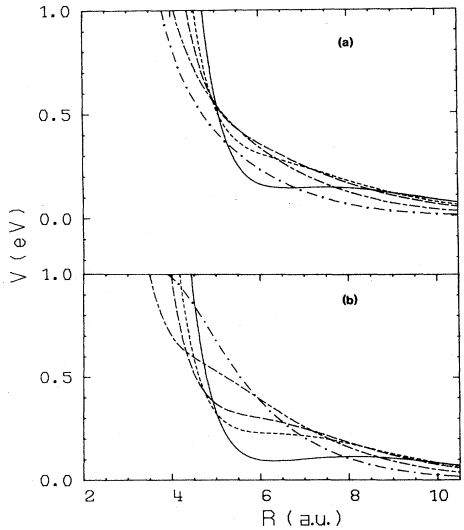

FIG. 21. Interaction potentials $V(R)$ for the $B^2\Sigma^+$ (a) and B^2A_1 (b) states of the M-H_2 systems. —·—·—·, Li; —·—·—, Na; ————, K; — — —, Rb; ——, Cs.

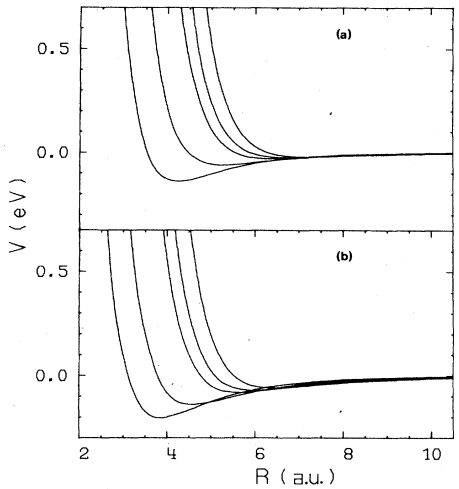

FIG. 22. Interaction potentials $V(R)$ for the $A^2\Pi$ (a) and A^2B_1 (b) states of the M-H_2 systems, as in Fig. 20.

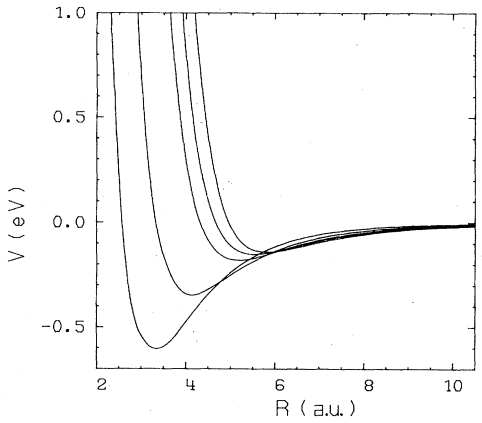

FIG. 23. Interaction potentials $V(R)$ for the A^2B_2 states of the M-H_2 systems, as in Fig. 20.

curve is observed for distances smaller than $R \simeq 4$ a.u., corresponding to the well in the Li^+H_2 potential curve (see Fig. 4). The $B^2\Sigma^+$ potential curves are attractive in R^{-5} and R^{-6}, while the B^2A_1 potential curves are repulsive in R^{-5} and R^{-6} by the term in $\alpha_{d_B}^{(2)}$, the term in $\alpha_{d_B}^{(0)}$ being attractive. However, for the $B^2\Sigma^+$ and B^2A_1 states, the repulsive interaction due to the overlap of the electronic densities contributes up to relatively large distances. Therefore, in Fig. 21 it is seen that the $B^2\Sigma^+$ potential curves are less repulsive than the B^2A_1 ones at large distances, while at short distances the order of the repulsive strength is changed because of the alkali-ion—H_2 interaction. At large distances, the $A^2\Pi$ potential curves are repulsive in R^{-5}, but then the terms in R^{-6} which are attractive become more important at shorter distances. The A^2B_1 and A^2B_2 potential curves are both attractive in R^{-5} and in R^{-6} by the term in $\alpha_{d_B}^{(0)}$ (which is the same as the one for the $A^2\Pi$ potential curve). The attractive strengths of the A^2B_2 potential curves is increased with respect to that of the A^2B_1 potential curves by different contributions in R^{-5}, and in R^{-6} by the term in $\alpha_{d_B}^{(2)}$. Because an M atom excited in a $nP_{\pm 1}$ state can approach more closely the H_2 molecule than it does when it is excited in a nP_0 state, and more closely in the C_{2v} symmetry than in the $C_{\infty v}$ symmetry, we find that the $A^2\Pi$, A^2B_1, and A^2B_2 potential curves have wells which are the deepest in the case of the A^2B_2 states. Finally, Table III summarizes the positions and the depths of the potential curves for the $X^2\Sigma^+$, X^2A_1, $A^2\Pi$, A^2B_1, and A^2B_2 states of all the M-H_2 systems. We note that comparatively, the depths of the ground-state potential curves of the M-H_2 systems are about a factor of 10 deeper than those for the M-He systems; and the $A^2\Pi$ potential curves of the M-H_2 systems have comparable well depths with the $A^2\Pi$ potential curves of the M-He systems.[1]

IV. CONCLUSIONS

Extensive molecular-structure calculations for all the M-H_2 systems in which H_2 is in its ground state $X^1\Sigma_g^+(v=0)$ have been made by using an l-dependent pseudopotential technique, and the adiabatic potential energies from the ground states up to highly excited levels have been obtained for the $C_{\infty v}$ and C_{2v} symmetries. The alkali-ion—H_2 interaction potentials have been also calculated. No experimental data are presently available for comparisons. However, comparisons with previous *ab initio* calculations performed at various levels of approximation have been possible, and good agreement has been obtained with the most sophisticated calculations. This indicates the reliability of our approach, which in other

TABLE III. Positions R_{eq} (in a.u.) and depths D_{eq} (in eV) of the $X^2\Sigma^+$, X^2A_1, $A^2\Pi$, A^2B_1, and A^2B_2 potential wells of the M-H_2 systems.

	$X^2\Sigma^+$		X^2A_1		$A^2\Pi$		A^2B_1		A^2B_2	
State	R_{eq}	D_{eq}	R_{eq}	D_{eq}	R_{eq}	D_{eq}	R_{eq}	D_{eq}	R_{eq}	D_{eq}
Alkali-metal										
Li	9.0	3.90×10^{-3}	10.4	1.87×10^{-3}	4.23	1.38×10^{-1}	3.90	1.98×10^{-1}	3.25	6.00×10^{-1}
Na	9.5	3.52×10^{-3}	10.5	1.83×10^{-3}	5.23	5.78×10^{-2}	4.55	1.38×10^{-1}	4.15	3.43×10^{-1}
K	11.4	2.02×10^{-3}	12.25	1.23×10^{-3}	6.33	2.89×10^{-2}	5.60	7.90×10^{-2}	5.18	1.80×10^{-1}
Rb	11.75	1.94×10^{-3}	12.75	1.20×10^{-3}	6.81	2.48×10^{-2}	6.0	7.02×10^{-2}	5.50	1.49×10^{-1}
Cs	12.60	1.61×10^{-3}	13.40	1.04×10^{-3}	7.25	2.07×10^{-2}	6.35	5.80×10^{-2}	5.80	1.40×10^{-1}

respects could be improved in the future, and gives us confidence in the predictions concerning those of the M-H_2 systems for which no information is available up to now. Extension of these calculations to the general C_s symmetry is only a question of additional computational efforts. A possible extension to slight variations of the $R_{H\text{-}H}$ distances is presently envisaged; however, this may not be sufficient for the study of the dynamics of some collisional processes, as it was shown to be in Ref. 11 where large positive deviations of $R_{H\text{-}H}$ were found to be important. The pseudopotential two-center approach could be also used to treat other systems, in particular the M-N_2 systems. Moreover, extension of the l-dependent pseudopotential approach to a three-center problem is anticipated for the future in view of treating reactive processes. Work is now in progress to use the present results in the study of some low-energy nonreactive collisional processes, in particular the fine-structure transitions in the first n^2P levels of the M atom and some intermultiplet transitions induced by collisions with H_2.

ACKNOWLEDGMENT

The authors wish to thank Professor J. R. Manson for a careful reading of the manuscript.

[1]J. Pascale, Phys. Rev. A **28**, 632 (1983).
[2]M. Krauss, J. Res. Natl. Bur. Stand., Sect. A **72**, 553 (1968).
[3]P. J. A. Ruttink and J. H. van Lenthe, Theor. Chim. Acta **44**, 97 (1977).
[4]A. F. Wagner, A. C. Wahl, A. M. Karo, and R. Krejci, J. Chem. Phys. **69**, 3756 (1978).
[5]K. Mizutani, Y. Kuribara, K. Hayashi, and S. Matsumoto, Bull. Chem. Soc. Jpn. **52**, 2184 (1979).
[6]P. Hobza and P. von R. Schleyer, Chem. Phys. Lett. **105**, 630 (1984).
[7]P. Botschwina, W. Meyer, I. V. Hertel, and W. Reiland, J. Chem. Phys. **75**, 5438 (1981).
[8]A. Sevin and P. Chaquin, Chem. Phys. **93**, 49 (1985).
[9]X. F. Gadea, G. H. Jeung, M. Pelissier, J. P. Malrieu, J. L. Picqué, G. Rahmat, J. Verges, and R. Vetter, Laser Chem. **2**, 361 (1983).
[10]J. C. Tully, J. Chem. Phys. **59**, 5122 (1973), and references therein.
[11]N. C. Blais, D. G. Truhlar, and B. C. Garrett, J. Chem. Phys. **78**, 2956 (1983), and references therein.
[12]See, for example, the review articles of J. D. Weeks, A. Hazi, and S. A. Rice, Adv. Chem. Phys. **16**, 283 (1969); J. N. Bardsley, Case Stud. At. Phys. **4**, 299 (1974); R. N. Dixon and I. L. Robertson, in *Theoretical Chemistry*, edited by Dixon and C. Thomson (Chemical Society, London, 1978), Vol. 3, p. 100.
[13]C. Bottcher, Chem. Phys. Lett. **35**, 367 (1975).
[14]A. D. Buckingham, Adv. Chem. Phys. **12**, 107 (1967).
[15]S. Hara, J. Phys. Soc. Jpn. **22**, 710 (1967).
[16]W. Kolos and L. Wolniewicz, J. Chem. Phys. **46**, 1426 (1967).
[17]G. Karl and J. D. Poll, J. Chem. Phys. **46**, 2944 (1967).
[18]K. Takayanagi and S. Geltman, Phys. Rev. A **138**, 1003 (1965).
[19]S. Sur and A. S. Ghosch, Phys. Rev. A **25**, 2519 (1982).
[20]F. Linder and H. Schmidt, Z. Naturforsch. Teil A **26**, 1603 (1971).
[21]E. S. Chang, J. Phys. B **14**, 893 (1981).
[22]G. Peach, in *Atoms in Astrophysics*, edited by P. G. Burke, W. B. Eissner, D. G. Hummer, and I. C. Percival (Plenum, New York, 1983), Chap. 5, and references therein.
[23]H. Inouye and S. Kita, J. Chem. Phys. **59**, 6656 (1973).
[24]J. C. Slater and J. G. Kirkwood, Phys. Rev. **37**, 682 (1931).
[25]See, for example, R. L. Flurry, Jr., in *Quantum Chemistry* (Prentice-Hall, Englewood Cliffs, 1983), p. 71.
[26]W. A. Lester, Jr., J. Chem. Phys. **54**, 3171 (1971).
[27]W. Kutzelnigg, V. Staemmler, and C. Hoheisel, Chem. Phys. **1**, 27 (1973).
[28]R. Raffenetti and K. Ruedenberg, J. Chem. Phys. **59**, 5978 (1973).
[29]J. B. Collins, P. von R. Schleyer, J. S. Binkley, J. A. Pople, and L. Radom, J. Am. Chem. Soc. **98**, 3436 (1976).
[30]J. D. Switalski, J. T. J. Huang, and M. E. Schwartz, J. Chem. Phys. **60**, 2252 (1974).
[31]E. Fermi, Nuovo Cimento **11**, 157 (1934).
[32]G. K. Ivanov, Teor. Eksp. Khim. **15**, 115 (1979).